文章编号: 1000-0615(2018)12-1896-10 DOI: 10.11964/jfc.20180111121

嘉陵江不同江段蛇鮈耳石形态特征及差异

彭 艳[1]， 曾 燏[1*]， 张 臣[1]， 龚建涵[1]， 周小云[1,2*]

(1. 西华师范大学生命科学学院，国家淡水渔业工程技术研究中心西南分中心，四川 南充 637009；
2. 华中农业大学水产学院，农业部淡水生物繁育重点实验室，湖北 武汉 430070)

摘要： 为研究蛇鮈耳石的形态特征以及不同环境下的耳石形态差异，以蛇鮈左侧微耳石和星耳石作为研究材料，利用传统形态法测量耳石的14个参数且将其转化为11个形状指标，并利用地标点法在星耳石上选取12个地标点，对2016年6—7月间采自嘉陵江上游、中游、下游的195尾蛇鮈的耳石样本进行形态研究。结果显示，蛇鮈微耳石呈肾形，3个江段微耳石形态无显著差异；蛇鮈星耳石呈圆形、椭圆形，表面粗糙，脊突数少于20，翼叶较基叶发达，中央突不明显，主凹槽轮廓似水滴状。相对扭曲主成分分析将3个江段的蛇鮈星耳石分为两种形态类型：Ⅰ型和Ⅱ型，其中Ⅰ型主要为嘉陵江上游江段蛇鮈的耳石样本，Ⅱ型则包括嘉陵江中游和下游的蛇鮈耳石样本。传统形态法和地标点法的综合结果表明，两种类型耳石形态差异主要表现在整体轮廓、脊突数，以及基叶、主凹槽和背侧距离等特征上，逐步判别分析对Ⅰ型和Ⅱ型星耳石的正判率达95.5%，区分效果较好。研究表明，嘉陵江不同江段蛇鮈星耳石分为两种类型，且存在显著的形态差异；蛇鮈星耳石的形态差异可能是对水温、流速等环境因子主动适应的结果，如在上游生活的蛇鮈，其较细长且脊突较多的Ⅰ型星耳石能够较好地适应上游低温、多变的急流环境。

关键词: 蛇鮈；耳石；形态特征；形态差异；环境适应；嘉陵江

中图分类号: Q 958.8; S 917.4 **文献标志码:** A

形态特征是生物体与生活环境长期相互作用的结果[1]，探讨生物体形态在不同环境下的差异及相互关系已成为现代生物学研究热点之一[2-3]，如国内外学者对鱼类的眼部[4]、口角须[5]以及头部[6]等外部形态与环境的适应关系作了深入研究。耳石(otolith)是鱼类感受声音和保持平衡的重要器官[7]，在不同生境下其形态会出现适应性变化[8-10]，如栖息中上层的南极鱼类较底栖南极鱼类拥有更圆的矢耳石轮廓[9]；同生活在低盐度环境条件的银汉鱼(*Odontesthes bonariensis*)相比，适应于高盐度环境的银汉鱼耳石形态更细长，主凹槽与耳石的周长之比也较小[11]。

鲤科(Cyprinidae)鱼类的耳石共3对，位于头骨后方，由碳酸钙组成[12]，其中矢耳石多细长易断[13]，微耳石和星耳石年轮清晰，常用作鱼类年龄鉴定[14-16]、物种及种群识别[13，17]等研究材料。传统的耳石形态学分析[18]主要利用耳石的线性测量距离去度量其外部形态，其易受人为因素影响，且结果单一，无法准确全面地对耳石形态进行描述；近年来结合二维图像的地标点法[19]日益受到重视，其通过地标点X、Y的坐标数据值，求出样本总体的平均形，对其进行相对扭曲主成分分析(relative warps，RW)，并绘制网格变形图，从而获取耳石形态差异的多元统计结果，其反映的耳石形态差异更全面可靠[20-21]。

蛇鮈(*Saurogobio dabryi*)，隶属于鲤科(Cyprinidae)鮈亚科(Gobioninae)蛇鮈属(*Saurogobio*)，

收稿日期： 2018-01-03 **修回日期：** 2018-04-25
资助项目： 国家自然科学基金(31472267, 513091960)；四川教育厅成果转化重大培养项目(17CZ0035)
通信作者： 曾燏，E-mail：zengyu@cwnu.edu.cn；周小云，E-mail：zhouxy@mail.hzau.edu.cn

是嘉陵江重要的小型经济鱼类，广泛分布于各江段，喜欢在沙质和卵石底质的微流水环境中集群产卵[22]。以往对于蛇鮈的研究主要集中在性腺发育[23]、两性异形[24]及肠道形态[25]等方面，目前有关耳石的研究多集中在海洋鱼类[26-27]，见诸报道的淡水鱼类耳石研究仅限于年龄判别[15]和物种鉴定[17]上，而涉及到蛇鮈耳石形态的研究更鲜有报道。本实验选取嘉陵江干流上游、中游和下游蛇鮈的星耳石和微耳石作为研究材料，结合传统形态学方法和地标点法分析不同江段蛇鮈的耳石形态特征及差异，并探讨其对环境的差异性适应。

1　材料与方法

于2016年6—7月在嘉陵江上游(广元段)、中游(蓬安段)、下游(合川段)3个江段共采集蛇鮈样本195尾，采样基本信息见表1。采回样本用10%的福尔马林溶液固定，带回实验室进行常规生物学测定，摘取耳石并清洗表面包膜，常温保存于1.5 mL的离心管中。

表 1　采样点及蛇鮈样本信息

Tab. 1　Sampling informations of locations and *S. dabryi*

采样点 sampling locations		平均水温/°C mean water temperature	平均流速/(m/s) mean flow velocity	星耳石 asteriscus	微耳石 lapillus	体长/mm body length
上游(广元段)	upstream(Guangyuan section)	25.3	0.35	72	68	136.09±14.56
中游(蓬安段)	midstream(Peng'an section)	27.2	0.11	44	40	128.55±9.95
下游(合川段)	downstream(Hechuan section)	29.1	0.05	79	45	114.95±11.52

注：采用浮标法测量采样点的流速
Notes: the flow velocity of sampling points were measured by float method

1.1　耳石形态测量

本研究以左侧星耳石和微耳石为研究材料，参照已有文献[28]的耳石形态描述和度量指标，使用TpsDig2软件测量耳石的长、高、面积、周长、基叶、翼叶等参数，鉴于蛇鮈耳石的测量指标可能存在体长效应[29]，因此利用SPSS 20.0软件将其转换为幅形比、圆度、形态因子、环率、矩形趋近率、椭圆率等形状指标列入单因素方差分析。耳石形态及测量性状如图1所示。

1.2　几何形态学测量分析

地标点的选取　以蛇鮈左侧星耳石作为研究材料，主要围绕基叶、翼叶、主凹槽建立地标点。生物学上将地标点分为三大类，其选取要求和具体操作见文献描述[19]，本实验参考类似研究[30]并结合蛇鮈星耳石的结构特点，选取了12个地标点(图1-b)。利用tpsDig2软件完成地标点选择工作，同时通过获取的12个地标点的全部X、Y坐标值建立相应的坐标点数据文件。

相对扭曲主成分分析与网格变形　利用tpsSmall软件对地标点的有效性进行检验。用tpsRelw对地标点进行处理，得到样本总体的平均形，对其进行相对扭曲主成分分析，并保存结果中的相对扭曲得分矩阵(relative warp scores matrix)。利用MorphoJ软件获取3个江段蛇鮈星耳石的网格变形图，比较不同江段蛇鮈星耳石形态差异。

判别分析　利用tpsRelw软件生成的相对扭曲得分，在SPSS 20.0中通过逐步判别分析对3个江段蛇鮈星耳石进行判别。

2　结果

2.1　传统耳石形态测量结果

耳石形态描述　蛇鮈星耳石稍大于微耳石。星耳石圆形或椭圆形，表面粗糙，背侧伴有数量不等的脊突，脊突数少于20个，翼叶较基叶发达，中央突突起不明显，具有一轮廓近似水滴状的主凹槽，尾部直达耳石前端；微耳石近似肾形，表面光滑，仅腹部有一圆形晶状突(图2)。

不同江段耳石性状差异　单因素方差分析结果表明，不同江段的蛇鮈星耳石差异显著，而微耳石无明显差异，其中星耳石的幅形比(L/H)、椭圆率((L-H)/(L+H))、基叶与耳石长之比(LR/L)、脊突数为上游>下游>中游，翼叶与耳石长之比(LA/L)为上游>中游>下游，基叶距离耳

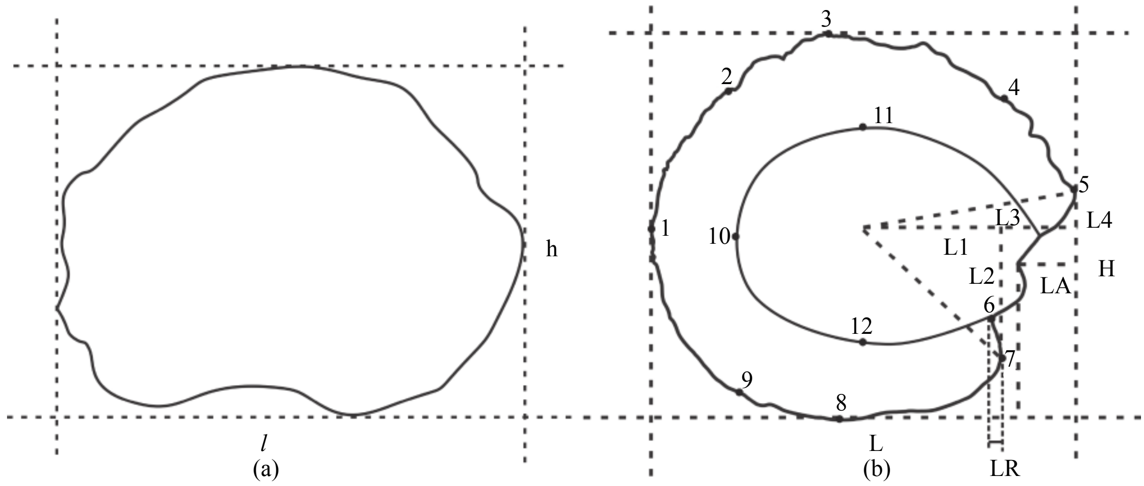

图 1　蛇鮈微耳石(a)和星耳石(b)测量示意图及地标点位置

测量指标：*l*.微耳石长；h.微耳石高；s.微耳石面积；p.微耳石周长；L.星耳石长；H.星耳石高；S.星耳石面积；P.星耳石周长；LR.基叶长；LA.翼叶长；L1.基叶距离星耳石中心的水平距离；L2.基叶距离星耳石中心的垂直距离；L3.翼叶距离星耳石中心的水平距离；L4.翼叶距离星耳石中心的垂直距离。形状指标：幅形比.l/h、L/H；圆度.$4s/\pi l^2$、$4S/\pi L^2$；形态因子：$4\pi s/p^2$、$4\pi S/P^2$；环率.p^2/s、P^2/S；矩形趋近率.$s/(l\times h)$、$S/(L\times H)$；椭圆率.$(l-h)/(l+h)$、$(L-H)/(L+H)$；LR/LA.基叶翼叶比；LR/L.基叶与耳石长之比；LA/L.翼叶与耳石长之比；L2/L1.基叶距离耳石中心距离的纵横比；L4/L3.翼叶距离耳石中心距离的纵横比；L/l.星、微耳石长度比；H/h.星、微耳石高度比；S/s.星、微耳石面积比；P/p.星、微耳石周长比。Ⅰ型地标点：6.基叶与翼叶或中央突的交点；10.主凹槽尾部的端点；11.主凹槽尾部和躯干部上交点；12.主凹槽尾部和躯干部下交点。Ⅱ型地标点：2.以地标点10为基点作垂线与背部的交点；4.以地标点7为基点作垂线与背部的交点；9.以地标点10为基点作垂线与腹部的交点。Ⅲ型地标点：1.耳石后端的最长点；3.耳石背侧的最宽点；5.耳石前端的最长点；7.基叶的端点；8.耳石腹侧的最宽点

Fig. 1　Measurements of *S. dabryi* lapillus(a), asteriscus(b) and locations of landmarks

Measure indices: *l*. lapillus length; h. lapillus height; s. lapillus area; p. lapillus perimeter; L. asteriscus length; H. asteriscus height; S. asteriscus area; P. asteriscus perimeter; LR. rostrum length; LA. antirostrum length; L1. horizontal distance from rostrum to the center of asteriscus; L2. vertical distance from rostrum to the core of asteriscus; L3. horizontal distance from antirostrum to the core of asteriscus; L4. vertical distance from antirostrum to the core of asteriscus. Shape indices: aspect ratio. l/h, L/H, roundness. $4s/\pi l^2$, $4S/\pi L^2$; format-factor. $4\pi s/p^2$, $4\pi S/P^2$; circularity. p^2/s, P^2/S; rectangularity. $s/(l\times h)$, $S/(L\times H)$; ellipticity. $(l-h)/(l+h)$, $(L-H)/(L+H)$; LR/LA. rostrum-to-antirostrum ratio; LR/L. rostrum -to- length ratio; LA/L. antirostrum-to-length ratio; L2/L1. aspect ratio of distance from rostrum to the asteriscus center; L4/L3. aspect ratio of distance from antirostrum to the asteriscus center; L/l. length ratio of asteriscus to lapillus; H/h. height ratio of asteriscus to lapillus; S/s. area ratio of asteriscus to lapillus; P/p. perimeter ratio of asteriscus to lapillus. Type Ⅰ landmark: 6. intersection of rostrum and antirostrum or central protrusion; 10. endpoint of sulcus tail; 11. upper intersection of sulcus tail and trunk; 12. lower intersection of sulcus tail and trunk. Type Ⅱ landmark: 2. intersection between the vertical line based on the landmark 10 and the dorsal side; 4. intersection between the vertical line based on the landmark 7 and the dorsal side; 9. intersection between the vertical line based on the landmark 10 and the ventral side. Type Ⅲ landmark: 1. the longest point of backend; 3. the widest point of dorsal side; 5. the longest point of forehead; 7. endpoint of rostrum; 8. the widest point of ventral side

石中心的纵横比(L2/L1)为上游<中游<下游。且上游与中、下游的以上性状差异均显著(P<0.05)，而中游与下游的性状(除L2/L1外)差异均不显著(P>0.05)(图3，表2)。

2.2　几何形态学分析

利用tpsRelw软件根据总体样本的地标点数据求出3个江段蛇鮈星耳石的平均形，并将所有地标点重叠矢量化，据此对其进行相对扭曲主成分分析，共提取20个主成分，其中第1主成分贡献率为43.71%，第2、3主成分分别贡献14.98%、6.41%，前3个主成分累积贡献65.10%。第1、2主成分的散点图显示，中游和下游样本重叠较多，在PC1、PC2上均无法分开，上游与中、下游样本在PC1上可较好分开(图4)，据此将嘉陵江蛇鮈星耳石分为两个类型，上游蛇鮈星耳石为Ⅰ型，中、下游为Ⅱ型。

在相对扭曲时，12个地标点中Ⅰ型地标点(6、10、11、12)和Ⅲ型地标点(1、3、5、7、8)的累积贡献率分别为51.23%、43.82%，Ⅱ型地标点2、4、9的贡献率仅4.95%(表3)，表明Ⅰ型和Ⅲ型地标点对区分不同江段蛇鮈耳石形态的作用较大。相对于样本总体的网格平均形，地标点6、7、8、10、11、12在3个江段蛇鮈星耳石的

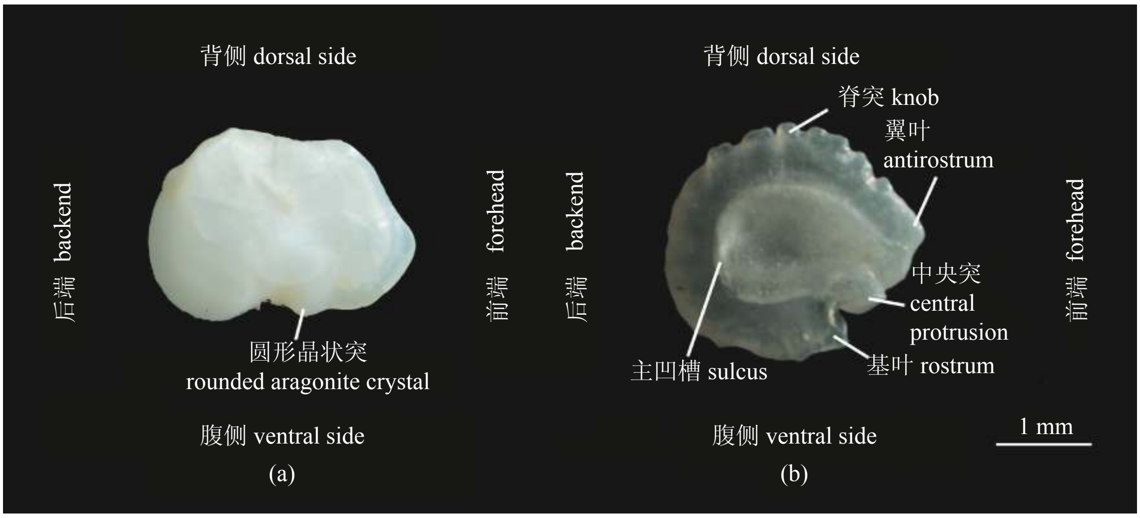

图 2　蛇鮈微耳石(a)、星耳石(b)形态示意图

Fig. 2　Shape of lapillus(a) and asteriscus(b) of *S. dabryi*

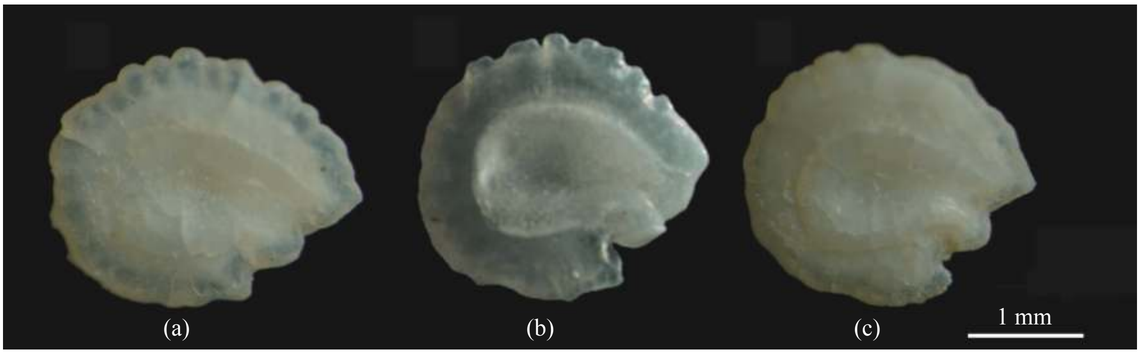

图 3　不同江段蛇鮈星耳石形态

(a)上游(广元段)；(b)中游(蓬安段)；(c)下游(合川段)，下同

Fig. 3　The asteriscus morphometry of *S. dabryi* in three sections

(a) upstream(Guangyuan section); (b) midstream(Peng'an section); (c) downstream(Hechuan section), the same below

表 2　蛇鮈星耳石的形态性状

Tab. 2　The morphological characters of *S. dabryi* asteriscus

性状 character	上游 upstream	中游 midstream	下游 downstream
幅形比　aspect ratio	1.156±0.007^{a}	1.106±0.008^{b}	1.121±0.006^{b}
椭圆率　ellipticity	0.071±0.003^{a}	0.048±0.005^{b}	0.057±0.002^{b}
基叶比耳石长　LR/L	0.113±0.002^{a}	0.096±0.002^{b}	0.097±0.002^{b}
翼叶比耳石长　LA/L	0.174±0.002^{a}	0.160±0.002^{b}	0.155±0.002^{b}
基叶距离耳石中心的纵横比　L2/L1	0.880±0.015^{a}	1.083±0.021^{b}	1.339±0.025^{c}
脊突数/个　knobs number	6.050±0.279^{a}	4.500±0.257^{b}	4.830±0.172^{b}

注：数据采用平均值±标准误，不同江段同行数据的不同字母表示差异显著(P<0.05)

Notes: the data were presented by the mean±SE, and the different letters meant significant difference(P<0.05)

网格扭曲中变形较大(图5)，表明不同江段蛇鮈星耳石形态差异主要表现在基叶(地标点6、7)、主凹槽(地标点10、11、12)，以及腹侧最宽点(地标点8)。

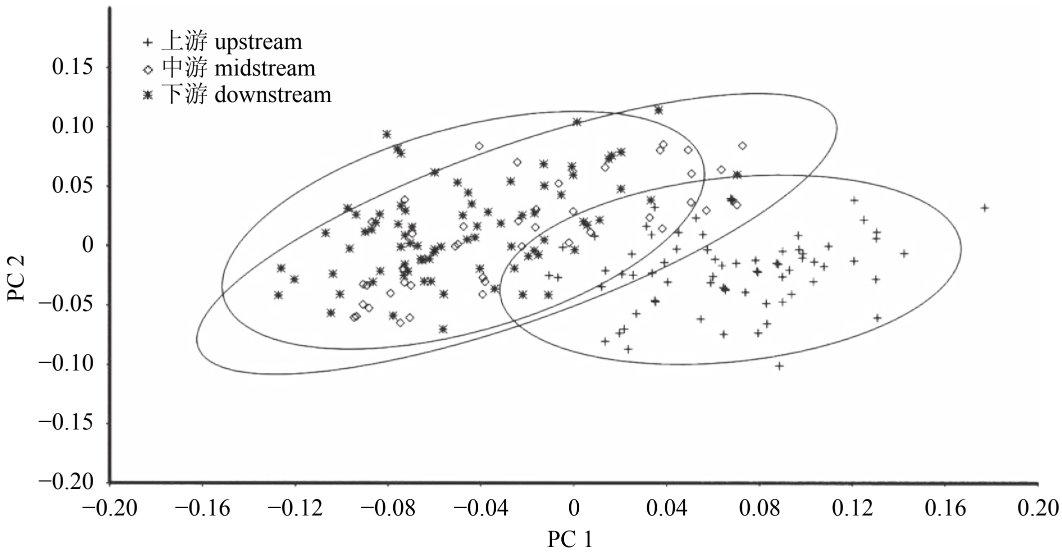

图 4 3个江段蛇鮈星耳石相对扭曲第1、2主成分散点图

Fig. 4 Scatter plots of relative warp scores on the 1st and 2nd for *S. dabryi* asteriscus of three sections

表 3 不同地标点在相对扭曲分析时的贡献率

Tab. 3 Contribution rate of twelve landmarks to relative warps %

地标点 landmark	贡献率 contribution rate
1	2.32
2	1.44
3	2.46
4	1.40
5	1.59
6	39.06
7	32.72
8	4.74
9	2.11
10	4.83
11	3.19
12	4.15

2.3 判别分析

对3个江段蛇鮈星耳石的20个相对扭曲得分进行逐步判别分析，根据对模型的预测贡献力逐步剔除不相关变量，最终6个变量(RW1、RW2、RW3、RW4、RW12、RW15)纳入判别分析，判别函数方程：

上游(广元段)：Y_1=67.114X_1−49.003X_2−15.960X_3−36.763X_4+28.776X_5+ 62.648X_6−4.157

中游(蓬安段)：Y_2=−17.189X_1+ 15.230X_2−46:414X_3+23.467X_4+ 33.031X_5−62.415X_6−2.218

下游(合川段)：Y_3=−47.391X_1+29.156X_2+46.708X_3+19.750X_4−40.457X_5−31.622X_6−2.767

式中X_1为RW1；X_2为RW2；X_3为RW3；X_4为RW4；X_5为RW12；X_6为RW15。

将195个样本代入判别方程，判别结果表明，上游72尾样本中，有6尾被错判，中下游两个江段123尾样本中仅1尾被错判为上游(表4)，根据主成分分析对蛇鮈星耳石的分类，Ⅰ型和Ⅱ型的正判率分别为91.7%和99.2%，综合正判率为95.5%。

3 讨论

嘉陵江蛇鮈微耳石似肾形，表面光滑，星耳石呈圆形或椭圆形，表面粗糙具数量不等的脊突，且不同江段间星耳石存在显著的形态差异(表2)。传统形态学和几何形态学分析结果表明，嘉陵江蛇鮈星耳石存在两种不同的形态类型(图3，图4)，如上游江段的Ⅰ型星耳石轮廓接近于椭圆形(即轮廓伸长)，基叶偏离耳石中心的角度相对较小；而中游和下游江段的Ⅱ型星耳石趋近于圆形，基叶偏离耳石中心的角度相对较大；Ⅰ型星耳石背侧的脊突个数较Ⅱ型多，主凹槽较Ⅱ型窄(图3)。相似的形态特征分化现象在其他鱼类的外部形态中也得到印证[4，6]，如在珠江流域不同江段的大眼鳜(*Siniperca kneri*)[31]

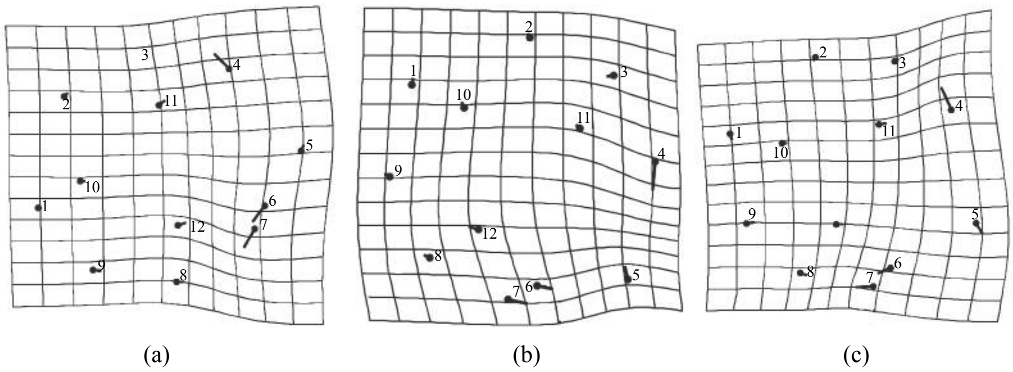

图 5　3个江段蛇鮈星耳石网格变形图

Fig. 5　Grid deformation for *S. dabryi* asteriscus of three sections

表 4　蛇鮈星耳石的判别结果

Tab. 4　Discriminant results of *S. dabryi* asteriscus

耳石类型 otolith type	采样点 sampling locations	判别正确率/% discrimination accuracy	判别结果/尾 discriminate result 上游(广元段) upstream (Guangyuan section)	中游(蓬安段) midstream (Peng'an section)	下游(合川段) downstream (Hechuan section)	合计 total
Ⅰ型 Type Ⅰ	上游(广元段) upstream(Guangyuan section)	91.7	66	3	3	72
Ⅱ型 Type Ⅱ	中游(蓬安段) midstream(Peng'an section)	81.8	1	36	7	44
	下游(合川段) downstream(Hechuan section)	91.1	0	7	72	79

中，其头部和尾部形态出现了显著性差异。

同时，不同江段蛇鮈星耳石形态的相对扭曲主成分分析显示，12个地标点中，6、7、10、8、12和11等6个地标点的累积贡献率高达88.69%，表明不同江段蛇鮈星耳石形态差异主要表现在星耳石的基叶、主凹槽和腹侧最宽点等3个特征上，这些形态指标可以作为今后开展鱼类耳石形态分析的主要候选指标。

耳石是控制鱼类听觉和平衡的重要器官[7]，其形态特征与生活环境密切相关[32-35]。如在流速快的深海水域的海洋鱼类中，耳石呈现出流线型，而流速较慢的沿海水域的同种鱼类耳石轮廓则趋于圆形[9，36]，且Bardarson等[10]指出鱼类流线型耳石形态的出现可能同鱼类流线型体型[37]对急流环境中游泳和觅食活动的适应原因相似。本研究的形态分析表明，同中游和下游江段的Ⅱ型星耳石形态相比，上游的Ⅰ型星耳石更显修长(图3，表2)，且实测数据表明，上游流速也较中、下游高(表1)，因此，推测较修长的I型星耳石形态是蛇鮈对嘉陵江上游较高流速环境的适应性结果。同时研究结果还发现蛇鮈星耳石背侧的脊突数量在两种类型耳石中也存在明显差异，其中Ⅰ型星耳石的突起数量多于Ⅱ型星耳石，认为较多的耳石突起有助于蛇鮈更灵敏地感应上游水流的快速变化。

耳石形态差异也可能与鱼类生长早期耳石不同区域的异速生长有关[35，38]，如严太明等[39]在相关研究中指出，鱼类早期耳石的前后区生长速率高于背腹区。本研究发现，Ⅰ型蛇鮈星耳石长高比大于Ⅱ型，且差异显著(P<0.05)(图3，表2)，这可能是蛇鮈对嘉陵江不同江段水温差异的适应结果。在嘉陵江上游，因水温较低(表1)，蛇鮈性成熟时间晚，其耳石的生长期较中游和下游长[40]，并最终导致上游Ⅰ型蛇鮈星耳石的长高比大于中游和下游的Ⅱ型星耳石。

鱼类耳石具有物种特异性，如耳石的基叶、主凹槽等局部形态特征[41]常被用于鱼类物种识别的研究[42-44]。然而，本研究结果表明，嘉陵江不同江段蛇鮈耳石存在显著的江段差异，表明耳石形态并不适合作为蛇鮈物种鉴定的主要依据。本研究从形态角度探讨蛇鮈耳石与嘉陵江不同江段的适应关系，为探讨生物体与环境

关系提供了新的例证。但鱼类耳石形态受遗传因素[45]与环境因素[34]共同影响，不同种类、环境，甚至不同性别等如何影响耳石形态仍待进一步研究。

参考文献：

[1] Blob R W, Bridges W C, Ptacek M B, *et al*. Morphological selection in an extreme flow environment: Body shape and waterfall-climbing success in the Hawaiian stream fish *Sicyopterus stimpsoni*[J]. Integrative and Comparative Biology, 2008, 48(6): 734-749.

[2] Chown S L, Klok C J. Altitudinal body size clines: latitudinal effects associated with changing seasonality[J]. Ecography, 2003, 26(4): 445-455.

[3] McAdam B J, Grabowski T B, Marteinsdóttir G. Identification of stock components using morphological markers[J]. Journal of Fish Biology, 2012, 81(5): 1447-1462.

[4] Strecker U, Bernatchez L, Wilkens H. Genetic divergence between cave and surface populations of Astyanax in Mexico (Characidae, Teleostei)[J]. Molecular Ecology, 2003, 12(3): 699-710.

[5] Wang X Z, Liu H Z. Phylogenetic relationships of the Chinese cyprinid genus *Rhinogobio* Bleeker (Teleostei: Cyprinidae) based on sequences of the mitochondrial DNA control region, with comments on character adaptations[J]. Hydrobiologia, 2005, 532(1-3): 215-220.

[6] Gordeeva N V, Nanova O G. Application of geometric morphometrics for intraspecific variability analysis in mesopelagic fishes of Sternoptychidae and Myctophidae families[J]. Journal of Ichthyology, 2017, 57(1): 29-36.

[7] Popper A N, Ramcharitar J, Campana S E. Why otoliths? Insights from inner ear physiology and fisheries biology[J]. Marine and Freshwater Research, 2005, 56(5): 497-504.

[8] Lombarte A, Lleonart J. Otolith size changes related with body growth, habitat depth and temperature[J]. Environmental Biology of Fishes, 1993, 37(3): 297-306.

[9] Lombarte A, Palmer M, Matallanas J, *et al*. Ecomorphological trends and phylogenetic inertia of otolith sagittae in Nototheniidae[J]. Environmental Biology of Fishes, 2010, 89(3-4): 607-618.

[10] Bardarson H, McAdam B J, Thorsteinsson V, *et al*. Otolith shape differences between ecotypes of Icelandic cod (*Gadus morhua*) with known migratory behaviour inferred from data storage tags[J]. Canadian Journal of Fisheries and Aquatic Sciences, 2017, 74(12): 2122-2130.

[11] Avigliano E, Martinez C F R, Volpedo A V. Combined use of otolith microchemistry and morphometry as indicators of the habitat of the silverside (*Odontesthes bonariensis*) in a freshwater-estuarine environment[J]. Fisheries Research, 2014, 149: 55-60.

[12] Schulz-Mirbach T, Plath M. *Corrigendum* to: all good things come in threes-species delimitation through shape analysis of saccular, lagenar and utricular otoliths[J]. Marine and Freshwater Research, 2015, 66(8): 757.

[13] 张国华. 耳石形态和元素组成及其与鱼类群体识别的研究[D]. 武汉: 中国科学院水生生物研究所, 2000: 29.
Zhang G H. Otolith morphology and elemental composition with the application in stock discrimination of fish[D]. Wuhan: Institute of Hydrobiology, Chinese Academy of Sciences, 2000: 29(in Chinese).

[14] 沈建忠, 曹文宣, 崔奕波, 等. 鲫耳石重量与年龄的关系及其在年龄鉴定中的作用[J]. 水生生物学报, 2002, 26(6): 662-668.
Shen J Z, Cao W X, Cui Y B, *et al*. The relationship between otolith-weight and age with reference to its use in age determination for *Carassius auratus*[J]. Acta Hydrobiologica Sinica, 2002, 26(6): 662-668(in Chinese).

[15] 沈建忠, 曹文宣, 崔奕波. 鲫耳石年轮的观察及其确证[J]. 华中农业大学学报, 2002, 21(1): 64-68.
Shen J Z, Cao W X, Cui Y B. Observation and validation of annuli in otoliths of *Carassius auratus*[J]. Journal of Huazhong Agricultural University, 2002, 21(1): 64-68(in Chinese).

[16] 熊飞, 陈大庆, 刘绍平, 等. 青海湖裸鲤不同年龄鉴定材料的年轮特征[J]. 水生生物学报, 2006, 30(2): 185-191.
Xiong F, Chen D Q, Liu S P, *et al*. Annuli characteristics of the different ageing materials of *Gymnocypris przewalskii przewalskii* (Kessler)[J]. Acta Hydrobiologica Sinica, 2006, 30(2): 185-191(in Chinese).

[17] 王臣, 刘伟, 王继隆. 利用Matlab软件进行耳石形态实例研究[J]. 淡水渔业, 2015, 45(2): 24-29.
Wang C, Liu W, Wang J L. Case studies on otolith morphology using Matlab[J]. Freshwater Fisheries, 2015, 45(2): 24-29(in Chinese).

[18] 姜涛, 杨健, 刘洪波, 等. 刀鲚、凤鲚和湖鲚矢耳石的

形态学比较研究[J]. 海洋科学, 2011, 35(3): 23-31.
Jiang T, Yang J, Liu H B, *et al*. A comparative study of the morphology of sagittal otolith in *Coilia nasus*, *Coilia mystus* and *Coilia nasus taihuensis*[J]. Marine Sciences, 2011, 35(3): 23-31(in Chinese).

[19] Bookstein F L. Introduction to methods for landmark data[M]//Rohlf F J, Bookstein F L. Proceedings of the Michigan Morphometrics Workshop. Ann Arbor: University of Michigan Museum of Zoology Special Publication, 1990: 215-226.

[20] 侯刚, 王学锋, 朱立新, 等. 基于几何形态测量学的4种金线鱼矢耳石识别研究[J]. 海洋与湖沼, 2014, 45(3): 496-503.
Hou G, Wang X F, Zhu L X, *et al*. Geometric morphometrics of sagittal otolith of four *Nemipterus* fish species[J]. Oceanologia et Limnologia Sinica, 2014, 45(3): 496-503(in Chinese).

[21] Monteiro L R, Di Beneditto A P M, Guillermo L H, *et al*. Allometric changes and shape differentiation of sagitta otoliths in sciaenid fishes[J]. Fisheries Research, 2005, 74(1-3): 288-299.

[22] 何学福, 宋昭彬, 谢恩义. 蛇鮈的产卵习性及胚胎发育[J]. 西南师范大学学报(自然科学版), 1996, 21(3): 276-281.
He X F, Song Z B, Xie E Y. The breeding habits and embryonic development of longnose gudgeon (*Saurogobio dabryi* Bleeker)[J]. Journal of Southwest China Normal University (Natural Science), 1996, 21(3): 276-281(in Chinese).

[23] 周春花, 欧阳珊, 郭治之, 等. 繁殖季节蛇鮈性腺发育的研究[J]. 水利渔业, 2004, 24(5): 24-25.
Zhou C H, Ouyang S, Guo Z Z, *et al*. Study on gonad development in breeding season of *Saurogobio dabryi*[J]. Reservoir Fisheries, 2004, 24(5): 24-25(in Chinese).

[24] 胡月, 曾燏, 蒋朝明, 等. 嘉陵江下游蛇鮈的两性异形与雌性个体生殖力[J]. 应用生态学报, 2017, 28(2): 658-664.
Hu Y, Zeng Y, Jiang Z M, *et al*. Sexual size dimorphism and female individual fecundity of *Saurogobio dabryi* in the lower reaches of the Jialing River, Southwest China[J]. Chinese Journal of Applied Ecology, 2017, 28(2): 658-664(in Chinese).

[25] 张臣, 曾燏, 彭艳, 等. 嘉陵江下游蛇鮈肠道形态结构及其异速生长模式[J]. 水产学报, 2018, 42(4): 503-512.
Zhang C, Zeng Y, Peng Y, *et al*. Morphological structure and allometric growth pattern of *Saurogobio dabryi* intestine in the lower reaches of Jialing River[J]. Journal of Fisheries of China, 2018, 42(4): 503-512(in Chinese).

[26] Lombarte A, Fortuño J M. Differences in morphological features of the sacculus of the inner ear of two hakes (*Merluccius capensis* and *M. paradoxus*, *Gadiformes*) inhabits from different depth of sea[J]. Journal of Morphology, 1992, 214(1): 97-107.

[27] Sadighzadeh Z, Valinassab T, Vosugi G, *et al*. Use of otolith shape for stock identification of John's snapper, *Lutjanus johnii* (Pisces: Lutjanidae), from the Persian Gulf and the Oman Sea[J]. Fisheries Research, 2014, 155: 59-63.

[28] 李辉华, 郭弘艺, 唐文乔, 等. 两种耳石分析法在鲚属种间和种群间识别效果的比较研究[J]. 淡水渔业, 2013, 43(1): 14-18.
Li H H, Guo H Y, Tang W Q, *et al*. Comparative study of two otolith shape analysis for genus *Coilla* species and stocks identification[J]. Freshwater Fisheries, 2013, 43(1): 14-18(in Chinese).

[29] 区又君, 廖锐, 李加儿, 等. 4种石首鱼耳石形态特征的比较[J]. 华南农业大学学报, 2012, 33(2): 203-210.
Qu Y J, Liao R, Li J E, *et al*. Comparison of morphological characteristics of otolith in four sciaenid fishes[J]. Journal of South China Agricultural University, 2012, 33(2): 203-210(in Chinese).

[30] 侯刚, 刘丹丹, 冯波, 等. 基于地标点几何形态测量法识别北部湾4种白姑鱼矢耳石形态[J]. 中国水产科学, 2013, 20(6): 1293-1302.
Hou G, Liu D D, Feng B, *et al*. Using landmark-based geometric morphometrics analysis to identify sagittal otolith of four *Pennahia* fish species[J]. Journal of Fishery Sciences of China, 2013, 20(6): 1293-1302(in Chinese).

[31] 杨慧荣, 欧阳徘徊, 李桂峰, 等. 珠江流域3个野生大眼鳜群体的形态差异[J]. 中国水产科学, 2016, 23(2): 447-457.
Yang H R, Ouyang P H, Li G F, *et al*. Morphological differentiation among three wild populations of *Siniperca kneri* in Pearl River[J]. Journal of Fishery Sciences of China, 2016, 23(2): 447-457(in Chinese).

[32] Gauldie R W. The morphology and periodic structures of

the otolith of the Chinook salmon (*Oncorhynchus tshawytscha*), and temperature-dependent variation in otolith microscopic growth increment width[J]. Acta Zoologica, 1991, 72(3): 159-179.

[33] Cardinale M, Doering-Arjes P, Kastowsky M, *et al*. Effects of sex, stock, and environment on the shape of known-age Atlantic cod (*Gadus morhua*) otoliths[J]. Canadian Journal of Fisheries and Aquatic Sciences, 2004, 61(2): 158-167.

[34] Tuset V M, Otero-Ferrer J L, Gómez-Zurita J, *et al*. Otolith shape lends support to the sensory drive hypothesis in rockfishes[J]. Journal of Evolutionary Biology, 2016, 29(10): 2083-2097.

[35] Vignon M. Ontogenetic trajectories of otolith shape during shift in habitat use: Interaction between otolith growth and environment[J]. Journal of Experimental Marine Biology and Ecology, 2012, 420-421: 26-32.

[36] Webb P W. Locomotor patterns in the evolution of actinopterygian fishes[J]. American Zoologist, 1982, 22(2): 329-342.

[37] Páez D J, Hedger R, Bernatchez L, *et al*. The morphological plastic response to water current velocity varies with age and sexual state in juvenile Atlantic salmon, *Salmo salar*[J]. Freshwater Biology, 2008, 53(8): 1544-1554.

[38] Meekan M G, Dodson J J, Good S P, *et al*. Otolith and fish size relationships, measurement error, and size-selective mortality during the early life of Atlantic salmon (*Salmo salar*)[J]. Canadian Journal of Fisheries and Aquatic Sciences, 1998, 55(7): 1663-1673.

[39] 严太明, 胡佳祥, 杨婷, 等. 骨唇黄河鱼耳石早期形态发育和轮纹特征研究[J]. 水生生物学报, 2014, 38(4): 764-771.

Yan T M, Hu J X, Yang T, *et al*. Study on the otolith development and the formation of increments in larvae and juvenile of *Chuanchia labiosa*[J]. Acta Hydrobiologica Sinica, 2014, 38(4): 764-771(in Chinese).

[40] 谢恩义. 蛇鮈个体生殖力的研究[J]. 怀化师专学报, 1997, 16(5): 58-60.

Xie E Y. Study on the individual fecundity of longnose gudgeon (*Saurogbio dabryi* Bleeker)[J]. Journal of Huaihua Teachers College, 1997, 16(5): 58-60(in Chinese).

[41] Avigliano E, Jawad L A, Volpedo A V. Assessment of the morphometry of saccular otoliths as a tool to identify triplefin species (Tripterygiidae)[J]. Journal of the Marine Biological Association of the United Kingdom, 2016, 96(5): 1167-1180.

[42] Reichenbacher B, Feulner G R, Schulz-Mirbach T. Geographic variation in otolith morphology among freshwater populations of *Aphanius dispar* (Teleostei, Cyprinodontiformes) from the southeastern Arabian Peninsula[J]. Journal of Morphology, 2009, 270(4): 469-484.

[43] Vignon M, Morat F. Environmental and genetic determinant of otolith shape revealed by a non-indigenous tropical fish[J]. Marine Ecology Progress Series, 2010, 411: 231-241.

[44] Teimori A, Jawad L A J, Al-Kharusi L H, *et al*. Late Pleistocene to Holocene diversification and historical zoogeography of the Arabian killifish (*Aphanius dispar*) inferred from otolith morphology[J]. Scientia Marina, 2012, 76(4): 637-645.

[45] Reichenbacher B, Reichard M. Otoliths of five extant species of the annual killifish *Nothobranchius* from the East African Savannah[J]. PLoS One, 2014, 9(11): e0124984.

Otolith morphology of *Saurogobio dabryi* and the variance in different sections of Jialing River

PENG Yan [1], ZENG Yu [1*], ZHANG Chen [1], GONG Jianhan [1], ZHOU Xiaoyun [1,2*]

(1. *Southwest Branch of the National Freshwater Fishery Engineering Technology Research Center*, *College of Life Science*, *China West Normal University*, *Nanchong* 637009, *China*;
2. *Key Laboratory of Freshwater Animal Breeding*, *Ministry of Agriculture*, *College of Fisheries*, *Huazhong Agricultural University*, *Wuhan* 430070, *China*)

Abstract: The purposes of this study were to understand the otolith morphology of *Saurogobio dabryi* in Jialing River, as well as its phenotypic consequences of water environments variations. 195 *S. dabryi* individuals were collected from the upper (Guangyuan section), middle (Peng'an section) and lower reaches (Hechuan section) of the Jialing River from June to July, 2016. The lapillus and asteriscus of the left side were used as the study materials. 14 morphometric parameters were measured with traditional methods and transformed into shape indices such as aspect ratio, roundness, format-factor, circularity, rectangularity, ellipticity, etc. Besides, 12 landmarks were established around the rostrum, antirostrum and sulcus of asteriscus by landmark methods. The results showed that the lapillus of *S. dabryi* was reniform, the morphology had no significant difference among three sections. the asteriscus of *S. dabryi* was round or oval with a rough surface, the number of knobs was less than 20, the antirostrum was more developed than rostrum, but the central protrusion was not very obvious, the sulcus was teardrop-shaped. Relative warp principal component analysis divided *S. dabryi* asteriscus of three sections into two types, Type Ⅰ and Type Ⅱ. Type Ⅰ contains the upstream of Jialing River *S. dabryi* asteriscus samples, while Type Ⅱ includes the middle and lower reaches of Jialing River *S. dabryi* asteriscus samples. The comprehensive results of traditional morphological method and landmark method showed the morphological differences of the two types were mainly reflected in the overall contour, the knob number, the basal leaf (landmark 6, 7), the sulcus (landmark 10, 11, 12) and the widest point of ventral side (landmark 8). The discriminant analysis results showed that the correct classification could reach 95.5% between two types. The asteriscus of *S. dabryi* from different river sections of Jialing River can be divided into two significantly different types, which may be related to the adaptation of environmental factors such as water temperature and flow velocity, for example, the slender asteriscus of Type Ⅰ with more knobs could be better adapted to the changeful rapids environment at low temperature of upstream.

Key words: *Saurogobio dabryi*; otolith; morphological characteristics; morphological difference; environmental adaptation; Jialing River

Corresponding author: ZENG Yu. E-mail: zengyu@cwnu.edu.cn;
ZHOU Xiaoyun. E-mail: zhouxy@mail.hzau.edu.cn

Funding projects: National Natural Science Foundation of China (31472267, 51779210); Major Cultivation Project of Education Department in Sichuan Province, China(17CZ0035)